NJC

PAPER

View Article Online
View Journal

Cite this: DOI: 10.1039/c8nj06120c

Superb-selective chemodosimetric signaling of sulfide in the absence and in the presence of CT-DNA and imaging in living cells by a plant alkaloid berberine analogue†

Gopal Chandra Jana,[a] Munira Khatun,[a] Sk Nayim,[a] Somnath Das,[a] Anukul Maji,[a] Maidul Beg,[a] Anirudha Patra,[a] Paromita Bhattacharjee,[b] Kakali Bhadra[b] and Maidul Hossain *[a]

The present manuscript reports a lucrative design of a colorimetric and ratiometric chemodosimeter, 9-*O*-(2,4-dinitrobenzenesulfonyl)berberrubine (BER-S), with excellent water solubility for the superb selective detection of sulfides through a color alteration from yellow to red with a good limit of detection (LOD) of 56 nM in CP buffer solution (10 mM, pH 7.2). Interestingly, this work also includes a smart "turn-on" emission probe (BER-S/DNA complex) showing good linearity with an excellent LOD of 46 nM for recognizing sulfide anions. The probes, BER-S, and BER-S/DNA complex, displayed no interfering effect by other analytes or sulfur-containing inorganic compounds, like thiols. Characterization was carried out using IR, HRMS, and DFT for the BER-S probe, and time-resolved fluorescence lifetime measurement and fluorescence titration for the BER-S/DNA complex probe for elucidating their sensing mechanism. The detection of S^{2-} in waste, tap, and drinking water by BER-S indicated its potential application in real sample analysis, while concentration variant cell imaging experiments (naked-eye red fluorescence) verified its cell-membrane permeability and capability for S^{2-} imaging in living cells. This reaction-based sensing strategy in the presence of DNA may provide a potential platform for the design of a fluorescent chemodosimeter for extensive anion targets.

Received 3rd December 2018,
Accepted 3rd January 2019

DOI: 10.1039/c8nj06120c

rsc.li/njc

1. Introduction

The design and development of efficient sensor systems to detect various chemically and biologically significant species has attracted considerable interest from researchers.[1] Recently, the potential of a high recognition and sensitive anion detection platform has drawn considerable attention for their vital roles in environmental, industrial, and biological processes.[1b] Being one of the most environmentally and biologically significant anions, sulfides are frequently used in various fields, for example, dyes and cosmetic manufacturing, for conversion into sulfuric acid, and in the production of wood pulp.[2] As a result, sulfide (S^{2-}) anions can be widely circulated in water *via* industrial processes and by the reduction of sulfate by anaerobic bacteria.[2] Besides, sulfides have a harmful effect on aquatic ecosystems and human beings, and their concentration is an essential aspect of the environmental index.[3] Sulfides can cause coma and respiratory paralysis, and even infuriate mucous membranes.[2,4] The protonated form of sulfides, *i.e.*, HS^- or H_2S, are more toxic than sulfides. H_2S at low concentration can produce individual distress; however, higher concentrations cause the loss of perception, eternal brain spoil, or even death through asphyxiation.[5] Furthermore, sulfides have emerged as a novel vital mediator in the cardiovascular organism, the nervous system, and in various biological signaling functions.[6] Therefore, it is challenging to develop a water-soluble, rapid, reliable, and sensitive probe for the detection of sulfide anions in aqueous medium and biological systems.

To date, many detection techniques have been developed for S^{2-} anions; for example, electrochemical methods,[7] ion chromatography,[8] titration,[9] inductively coupled plasma atomic emission spectroscopy,[10] spectrophotometry,[11] hydride generation atomic fluorescence spectrometry,[12] fluorometric,[13–17] and chemiluminescence.[18] While they offer high accuracy, these methods need complicated instrumentation, expert personnel, and time-consuming sample preparation, which make them inappropriate for real applications. The fluorescent sensing

[a] *Department of Chemistry and Chemical Technology, Vidyasagar University, Midnapore-721102, West Bengal, India. E-mail: hossainm@mail.vidyasagar.ac.in; Tel: +91-9432976277*

[b] *Department of Zoology, University of Kalyani, Kalyani-741235, West Bengal, India*

† Electronic supplementary information (ESI) available. See DOI: 10.1039/c8nj06120c

method has received great attention among these reported recognition methods due to its high sensitivity and simple operation.

Till now, many fluorescent probes have been successfully developed to detect sulfide anions.[19–27] However, most of these probes suffer from poor water solubility, *i.e.*, a mixture of water and the organic solvent is required for their better sensitivity, which limits their application in environmental and bio-related fields.[28–30] As a result, a lot of improvements are needed for sulfide anion detecting probes for potential environmental and biological applications, such as excellent water solubility and appliance in biological systems.[31–35]

The sulfide anion is an effective nucleophile and reacts readily with sulfonate esters or sulfonate ether compounds, and this fact tunes the idea for the design of a novel turn-on fluorescent chemodosimeter for S^{2-} anions.[36–41] In the recent literature, a few probes have been designed by splitting the dinitrophenyl ether or dinitrobenzenesulfonyl group to bring back their original fluorescence.[42–44] Thus, it was expected that incorporating the strong electron-withdrawing group dinitrobenzenesulfonate ester into a fluorophore could appreciably reduce the fluorescence, and then by cleaving it, a significant amplification in fluorescence intensity could be observed.[45–48]

More recently, a fluorescent DNA–gold/silver nano-clusters template was developed that allowed the discerning detection of sulfide anions, having a detection limit of 0.83 nM,[49] while another fluorescent sensor for the rapid detection of S^{2-} using dsDNA–CuNPs as fluorescent probes was also reported.[50] We recently developed a new sensing approach in the presence of DNA for hydrazine sensing with superb selectivity using a DNA–BER-BZ complex as a novel fluorescence probe.[51] In this system, hydrazine cleaved the ester bond of the probe to form an hydrazinolysed compound that also interacts with the DNA, and this interaction concomitantly causes a great rise in fluorescence intensity. Although the use of such a DNA–alkaloid complex in sensing has been barely studied, such potential emission probes have drawn immense attention for their potential biochemical impact. Thus, application of the DNA–alkaloid complex is of significant interest for sensing studies, particularly for application in highly selective and sensitive sulfide detection.

Inspired by the above perspective, we report herein a turn-on fluorescence sensor for S^{2-} ions using the BER-S/DNA complex. Accordingly, we synthesized a new 9-*O*-berberine derivative (BER-S, Scheme 1) by substituting the electron-withdrawing 2,4-dinitrosulfonyl group at the 9-O position in berberine. Owing to the presence of a sulfonate ester linkage at the 9 position, the probe acted as an excellent colorimetric chemodosimeter for sulfide anions in CP buffer medium (Scheme 1). The analogue BER-S could interact with DNA, and this binding phenomenon was investigated by various spectroscopic methods, such as UV-vis, fluorescence, fluorescence quenching, and viscosity measurements, which revealed that the analogue has a higher binding efficacy with CT-DNA than berberine. More interestingly, the probe in a DNA-binding situation (maximum saturation), *i.e.*, the BER-S/DNA complex, can act as a potential turn-on chemodosimetric fluorescence probe for the highly

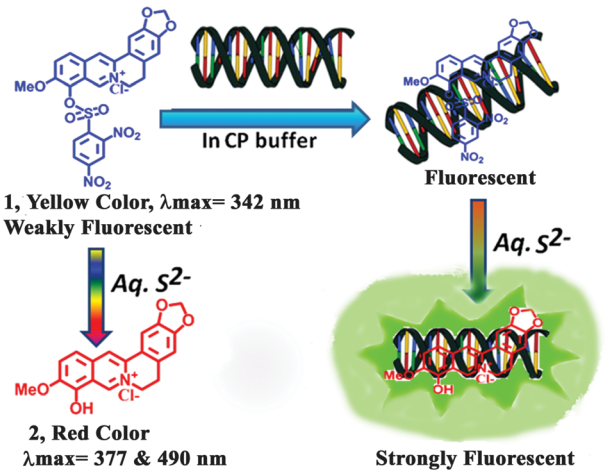

Scheme 1 Schematic of the proposed sensing mechanism in the absence of DNA and in the presence of DNA by BER-S.

selective detection of sulfide anions in CP buffer solution (10 mM, pH = 7.2) (Scheme 1). Additionally, concentration variant confocal microscopic imaging revealed that the BER-S was cell-permeable and sensed S^{2-} in the living cell. Thus, it heralds a new platform for the detection of sulfide anions by a DNA–alkaloid template and has unique biological value due to its ability to permeate the cell membrane and detect sulfide anions in a living cell.

2. Experimental section

2.1. Materials/chemicals and reagents

Berberine chloride (BC), sodium sulfide ($Na_2S{\cdot}10H_2O$), and calf thymus (CT) DNA (type XI, 42% guanine–cytosine content) were purchased from Sigma-Aldrich Corporation (St. Louis, MO, USA). Anionic salts (S^{2-}, Cl^-, Br^-, I^-, F^-, Ac^-, NO_2^-, NO_3^-, PO_4^{3-}, CN^-, SCN^-, HSO_3^-, SO_4^{2-}, SO_3^{2-}, $S_2O_3^{2-}$, $S_2O_8^{2-}$, HPO_4^{2-}, $H_2PO_4^-$, ClO_4^-, IO_4^-, $S_2O_8^{2-}$, BO_3^{3-}, $B_4O_7^{2-}$, N_3^-), cationic salts (Na^+, K^+, Ca^{2+}, Mg^{2+}, Pb^{2+}, Cu^{2+}, Fe^{3+}, Hg^{2+}, Zn^{2+}, Cd^{2+}, Co^{2+}), and life elements, such as ATP, GTP, ClO^-, H_2O_2, tyrosine, tryptophan, lysozyme, including biothiols (glutathione, cysteine, homocysteine, methionine, cysteamine, and thiobarbituric acid), and other solvents were obtained from Merck Pvt. Ltd (Singapore) and were used directly without further purification. The concentrations of BER-S and CT-DNA were determined by molar extinction coefficient (ε) values of 13 200 M^{-1} cm^{-1} at 260 nm and 19 000 M^{-1} cm^{-1} at 342 nm, respectively. The CT-DNA was dissolved in CP buffer solution (10 mM $[Na]^+$ at pH 7.2) and the purity of DNA was confirmed by monitoring the ratio of absorbance at 260/280 nm (A_{260}/A_{280}).

2.2. Instrumentation

^1H (500 MHz) and $^{13}C\{^1H\}$ (125 MHz) NMR spectra were recorded on a Bruker's AVANCE-III 500 MHz spectrometer in DMSO-d_6 solvent using TMS as an internal reference at 25 °C. Mass spectra of compound BER-S and mass spectral data for the sensing study were measured using a BrukermicroTOF QII

high-resolution mass spectrometer coupled to a Waters Acquity UPLC system. FT-IR spectra were measured with a PerkinElmer Spectrum, two FT-IR spectrophotometers equipped with a zinc selenide (ZnSe) attenuated total reflectance (ATR) accessory, $LiTaO_3$ detector, and a KBr beam splitter at ambient temperature (PerkinElmer, Inc., USA). UV-vis spectra were obtained from a Shimadzu UV-1601 spectrophotometer (Shimadzu Corporation, Kyoto, Japan). All the spectra were collected at 25 °C in quartz cuvettes of 1 cm path length. All the fluorescence spectra were measured on a PerkinElmer LS-55 (USA) spectrofluorimeter in fluorescence-free quartz cells of 1 cm path length. The widths of the excitation slit and emission slit were set to 2.5 nm and 5 nm, respectively.

The fluorescence lifetime data were collected using a DeltaFlex™ Moduler Fluorescence Lifetime system (Horiba Scientific, UK). The decay data were measured by the time-correlated single photon counting (TCSPC) procedure using CP buffer of pH 7.2 at an excitation wavelength of 372 nm from a laser LED source.

Density functional theory (DFT) and calculations *via* CAM-B3LYP/6-31g(d,p) level using the Gaussian 09 program were performed. A rotational viscometer (Brookfield, Middleboro, MA 02346, USA) armed with a 1 ml LCP spindle was used for the viscosity experiments, operating at 40 rpm at 25 °C.

2.3. Synthesis of berberrubine (2)

Commercially available berberine (**1**, 1 g) chloride was heated at 190 °C in a vacuum oven under reduced pressure of 20–30 mm Hg for 15 min to get berberrubine (**2**, 885 mg) in about a 90% yield according to previously reported work.[51]

2.4. Synthesis of 9-*O*-(2,4-dinitrobenzenesulfonyl)berberrubine (3)

First 2,4-dinitrobenzenesulfonyl chloride was added to the solution of **2** in CH_3CN, and then the reaction mixture was permitted to stir for 30 min at room temperature. The crude product was obtained by evaporating the solvent under vacuum and washed with diethyl ether. The product was purified through column chromatography on a silica gel column, eluted with varying concentrations of the $CHCl_3$–CH_3OH solvent mixture to get the desired product BER-S (**3**) as a yellow powder (80–85% yield), ^{1}H NMR (500 MHz, DMSO-d_6, TMS, 25 °C) δ = 3.22 (2H, t, J = 10), δ = 3.83 (3H, s), δ = 4.99 (2H, t, J = 7.5), δ = 6.18 (2H, s), δ = 7.11 (1H, s), δ = 7.18 (1H, s), δ = 8.10 (1H, d, J = 10), δ = 8.22 (1H, d, J = 10), δ = 8.32 (1H, d, J = 10), δ = 8.54 (1H, s), δ = 8.72 (1H, d, J = 10), δ = 9.16 (1H, s), δ = 9.65 (1H, s). ^{13}C NMR (125 MHz, DMSO-d_6, TMS, 25 °C) δ 29.83, 56.19, 59.24, 101.26, 103.14, 110.80, 112.68, 115.12, 118.81, 121.51, 124.26, 128.59, 131.96, 135.37, 137.52, 140.22, 142.74, 145.18, 146.99, 148.23, 151.02, 153.45, 156.24, 157.42. The values of ^{1}H, and ^{13}C NMR are in ppm units. UV/Vis (H_2O): 406, 342, 259 nm. HRLC-MS for $C_{25}H_{18}N_3O_{10}S$ calcd, 552.07, found 552.0765.

2.5. Procedure for spectral measurement for sulfide detection

The solutions of various analytes (1 mM) were prepared in Millipore water. The stock solution of the BER-S was prepared at 500 μM in Millipore water. The solution of BER-S was then diluted to 1 mM with CP buffer (10 mM, pH = 7.2). The titration experiments were carried out using 1 ml of BER-S (10 μM) stock solution of the probe, with BER-S in a quartz cell of 1 cm path length, and various analytes were gradually added by micropipette to record the spectrum. Spectrophotometric and spectrofluorimetric titrations of BER-S/DNA complex were performed taking solution (10 μM probe, 150 μM CT-DNA) in a quartz cell containing CP buffer (pH = 7. 2) with analyte solution added to record the spectra. For the fluorescence experiments, the excitation wavelength was fixed at 360 nm, and the emission was recorded from 400 to 700 nm.

2.6. Preparation of stock BER-S solution for the binding study

Stock solutions of BER-S were prepared in CP buffer solution and kept in the dark to avoid light-assisted photophysical changes. In this study, BER-S obeyed Beers' law in the experimental concentration range. The concentration of the BER-S solution was measured by the molar extinction coefficient (ε) value of 19 000 at 342 nm from the absorbance study.

2.7. Procedure for UV-vis and fluorescence spectral measurements for the binding study

The absorption titration experiments were carried out with gradually increasing the concentration of CT-DNA to a fixed concentration of BER-S. In general, to a solution of BER-S (10 μM) in 10 mM CP buffer were added aliquots of CT DNA in 10 mM CP buffer up to saturation, according to a previously reported protocol.[52] The emission titration was performed as dictated in the absorbance titration taking BER-S (10 μM) in 10 mM CP buffer solution.

2.8. Fluorescence quenching experiments

The fluorescence quenching experiment was performed with $K_4[Fe(CN)_6]$, an anionic quencher as per a previously reported protocol.[53] The $K_4[Fe(CN)_6]$ and KCl solutions were mixed in changed ratios to give a fixed total ionic strength. According to the Stern–Volmer equation, the data were plotted as the relative fluorescence intensity with varying concentration of the ferrocyanide at a constant P/D (CT-DNA/BER-S molar ratio) *versus* $[Fe(CN)_6]^{4-}$.

2.9. Viscosity measurements

To further inspect the binding mode of the BER-S with DNA, viscosity measurements were performed on CT-DNA with respect to varying concentrations of BER-S. The viscosities of a DNA solution (1 mM) were measured in the absence and presence of increasing concentrations of the BER-S (0.05–0.25 mM). The relation between the relative solution viscosity (η/η_0) and DNA length (L/L_0) is given by the following equation:[54]

$$L/L_0 = (\eta/\eta_0)^{1/3}$$

where L and L_0 denote the apparent molecular length in the presence and absence of the compound, respectively. The obtained data are presented as $(\eta/\eta_0)^{1/3}$ *versus* r, where η is the viscosity of DNA in the presence of BER-S, and η_0 is the

viscosity of DNA alone in a buffer solution, and r represents the ratio of [BER-S]/[DNA].

2.10. Analysis of the binding data

The UV-visible and fluorometric titrations were carried out in the range of 300–600 nm and 400–660 nm, respectively, in CP buffer solution to calculate the apparent binding constant from Scatchard plots of r/C_f *versus* r (where r is the number of moles of alkaloid analogue bound per mole of CT-DNA base pairs binding). The Scatchard plots showed a negative slope at higher r valued as observed in non-cooperative binding isotherms and therefore the binding affinity was analyzed by the following McGhee–von Hippel equation:[55]

$$\frac{r}{C_f} = K_i(1 - nr)[(1 - nr)/\{1 - (n - 1)r\}]^{n-1}$$

where K_i is the intrinsic binding constant to an isolated binding site and n is the number of base pairs excluded by the binding of a single alkaloid molecule. All the binding data were analyzed through the origin software, from which we calculated the best-fit parameters K_i and n.

2.11. Fluorescence quantum yield in solution

The fluorescence quantum yields of both the reactant (BER-S) and cleaved product (BER-OH) in the absence and presence of DNA were calculated in HPLC grade water using optically same solutions of quinine sulfate (Φ_r = 0.546 in 1 N H_2SO_4) as the standard at an excitation wavelength of 365 nm. The quantum yield was calculated using the following equation:[56]

$$\Phi_s = \Phi_r(A_rF_s/A_sF_r)(\eta_s^2/\eta_r^2)$$

where A_r and A_s are the absorbance of the reference and sample solutions, respectively, and F_r and F_s are the corresponding integrated fluorescence intensities (areas) at the same excitation wavelength, and η is the refractive index of the solvents.

2.12. Calculation of the detection limit

The detection limits of the probe BER-S and BER-S/DNA complex were calculated by the UV-vis titration and fluorescence titrations, respectively. To get the detection limit value, BER-S (10 μM) was titrated with an increasing concentration of S^{2-} (0–25 μM). Similarly, the BER-S/DNA complex was titrated with various concentration of S^{2-} (0–20 μM). The respective absorbance and fluorescence intensity of BER-S and BER-S/DNA complex were measured 10 times without S^{2-} anion, and the standard deviation of a blank measurement was obtained. To gain the slope, the absorbance ratio (A_{377}/A_{342}) and the emission intensity at 530 nm were plotted as a concentration of S^{2-}. Then, the detection limit was calculated with the following equation: detection limit = $3\sigma/k$, where σ is the standard deviation of blank measurement, and k is the slope between the absorbance ratios (A_{377}/A_{342}) and I_{530} *versus* [S^2].

2.13. Cytotoxicity assay

The A375 (skin melanoma) cell line was obtained from the National Centre for Cell Science, Pune. Cells were grown in DMEM medium supplemented with 10% heat-inactivated FBS and 1% antibiotic–antimycotic solution, in a CO_2 incubator at 37 °C with 5% CO_2. After culturing the cells (2×10^4 cells per 35 mm culture plate) for 24 h, the probe was added in various concentrations (5, 10, 15, 20, and 25 μM) and again after 48 h incubation. The percentage of viable cells was calculated as the IC_{50} (50% growth inhibition) values for the cell lines by MTT (1 mg ml^{-1} of the MTT) assay kit (Sigma), by the following formula:

$$IC_{50} = (T - T_0) \times 100/(C - T_0)$$

where T represents the optical density of the sample culture plate after 48 h of probe treatment, T_0 is the optical density at time zero, and C is the optical density of the control.

2.14. Fluorescence cell imaging

We performed the concentration variant fluorescence cell imaging experiment with the A375 (skin melanoma) cell line. After culturing the cells (2×10^4 cells per 35 mm culture plate) for 24 h, the various concentration of BER-S (3, 6, and 10 μM) was added in the three set of samples and after 30 min incubation, the images were obtained using an Invitrogen FL Digital Inverted Fluorescence Microscope (Invitrogen AMF 4300). Then the cells were treated with three different concentration of S^{2-} for 30 min interval for each set of samples and cell images were obtained using the same fluorescence microscope stated above. In all the cases, the red channel (540–644 nm wavelength range) was chosen to obtain the fluorescence images.

3. Results and discussion

3.1. Design and synthesis of BER-S

One of the most interesting features of the sulfide detector probe is that it contains a strong electron-withdrawing group, as already discussed in the Introduction section. Accordingly, we selected the 2,4-dinitrobenzenesulfonyl moiety for its well-known reactivity toward sulfide or thiols and utilized this as a sulfide detector probe in this article. Once the sulfonate is hydrolyzed by sulfide, it restores the color in the absence of DNA, while fluorescence can be observed in the presence of DNA.

As shown in Scheme 2, berberrubine (**2**) was synthesized by a selective demethylation reaction of berberine (**1**), followed by reaction with 2,4-dinitrobenzenesulfonylchloride in CH_3CN for about 30 min to produce the desired final product BER-S (**3**). The product was well characterized by ^1H, ^{13}C NMR, and TOF-MS (Fig. S20–S22, ESI†).

3.2. Spectral recognition study of S^{2-} by BER-S

3.2.1. UV-vis spectroscopic studies. The UV-vis spectra of BER-S in CP buffer solution (10 mM, pH = 7.2) exhibited an absorption maxima at 342 nm, which may due to π–π* electronic transition. Upon the gradual addition of S^{2-}, the absorption maxima at 342 nm gradually decreases, while a new peak at 377 nm gradually appears and additionally another new peak at 490 nm arises with one distinct isosbestic point (358 nm),

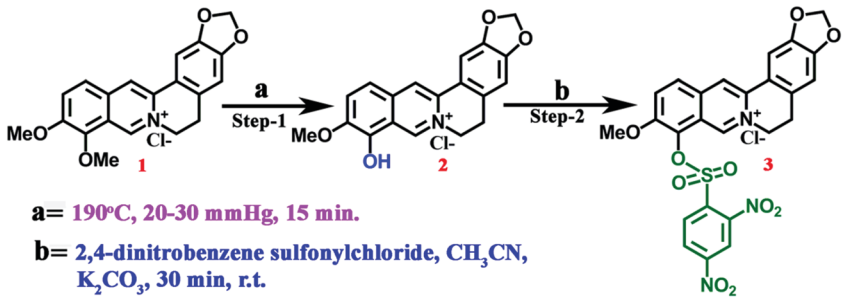

Scheme 2 Synthetic pathway for the synthesis of BER-S, **3**.

suggesting that two species are in equilibrium (Fig. 1a). Such a type of remarkable change in the absorption spectra (red-shift of 35 nm) allows the probe BER-S to be used for the colorimetric detection of S^{2-} anions with a color change from yellow to red (Fig. S4, ESI†). This is attributed by the nucleophilic attack of S^{2-} to the sulfonate ester linkage of the probe, removing the 2,4-dinitrobenzenesulfonyl group from the BER-S to produce berberrubine (**2**), and this structural change tunes the above changes in the electronic spectra. Accordingly, we plotted the absorbance ratio (A_{377}/A_{342}) *vs.* concentration of S^{2-}, which exhibited a nonlinear S like curve, and consequently a linear relationship was observed between A_{377}/A_{342} and the S^{2-} concentration in the range 0.0–1.2 μM with a correlation coefficient value $R^2 = 0.99235$ (Fig. 1b). Based on the IUPAC convention, the limit of detection value ($3\sigma/k$) was 56 nM, *i.e.*, much lower than the WHO permitted S^{2-} concentration in drinking water.[57] Thus, BER-S could be employed as a promising ratiometric chemodosimeter for the detection of S^{2-}.

3.2.2. Fluorescence study. Upon the successive addition of S^{2-} to the probe (10 μM), no remarkable change in the fluorescence spectra was observed, only a slight increase in the emission intensity (Fig. S5, ESI†). Hence, BER-S could not serve as a fluorescence turn-on probe for the detection of S^{2-}.

3.2.3. Selectivity, sensitivity, and competitive ion study. The superb selectivity of BER-S toward S^{2-} was evaluated by measuring the change in the UV-vis spectra in the absence and presence of S^{2-}. Almost no change in absorption ratio (A_{377}/A_{342}) was observed with the addition of environmentally and biologically rich anions like Cl^-, Br^-, I^-, F^-, Ac^-, NO_2^-, NO_3^-, PO_4^{3-}, CN^-, SCN^-, HSO_3^-, SO_4^{2-}, SO_3^{2-}, $S_2O_3^{2-}$, $S_2O_8^{2-}$, HPO_4^{2-}, $H_2PO_4^-$, ClO_4^-, IO_4^-, $S_2O_8^{2-}$, BO_3^{3-}, $B_4O_7^{2-}$, N_3^-, but upon the addition of S^{2-}, a drastic change in absorbance spectra were observed (Fig. S3, ESI†). We also checked the selectivity of our probe with the addition of cations, such as Ca^{2+}, Mg^{2+}, Fe^{3+}, Cu^{2+}, Zn^{2+}, Hg^{2+}, Cd^{2+}, Pb^{2+}, Co^{2+}, Na^+, K^+, and other life elements, like ATP, GTP, ClO^-, H_2O_2, tryptophan, trypsin, lysozyme, and accordingly no abrupt change in absorption was observed (Fig. S5 and S6, ESI†). These results are consistent with our expectation that the sulfonate ester group can selectively be cleaved by S^{2-} only, not by other ions.

Interestingly, we also examined whether the absorbance ratio changed or not in the presence of biological thiols, *i.e.*, glutathione (GSH), cysteine (Cys), homocysteine (Hcy), methionine (Met), cysteamine (Cyt), and thiobarbituric acid (TBA). However, no remarkable change in absorption spectra was observed in the presence of the thiol (Fig. S7, ESI†). Owing to the greater nucleophilicity of S^{2-} compared with GSH, Cys, Hcy, Met, Cyt, and TBA can

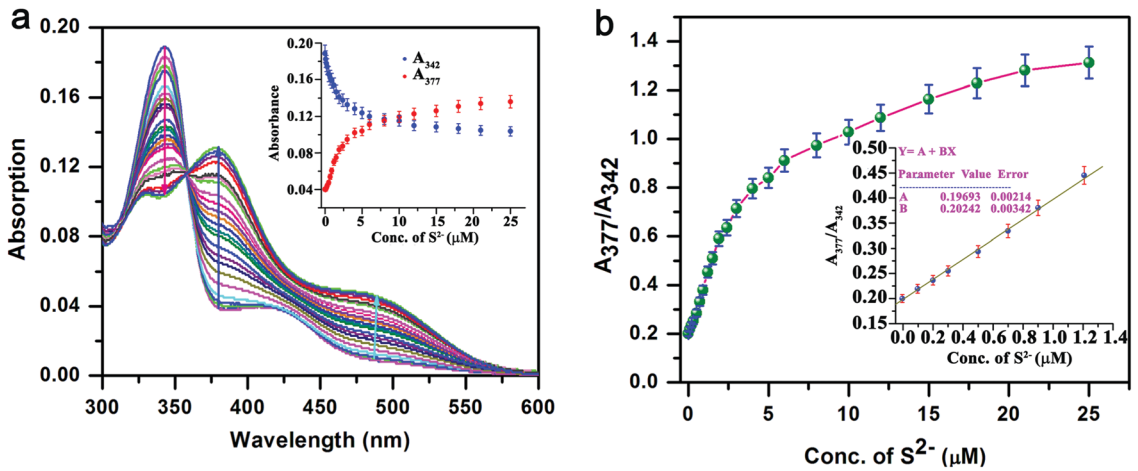

Fig. 1 UV-vis spectra of BER-S (10 μM) (a) with increasing concentration of sulfide (0–2.5 equiv.). (b) The plot of absorption ratios at 377 nm and 342 nm of BER-S (10 μM) upon the addition of varied concentrations of sulfide (0–25 μM), where the absorption ratio of BER-S (10 μM) was linearly related to the concentration of sulfide (0.0–1.2 μM) in CP buffer solution (inset).

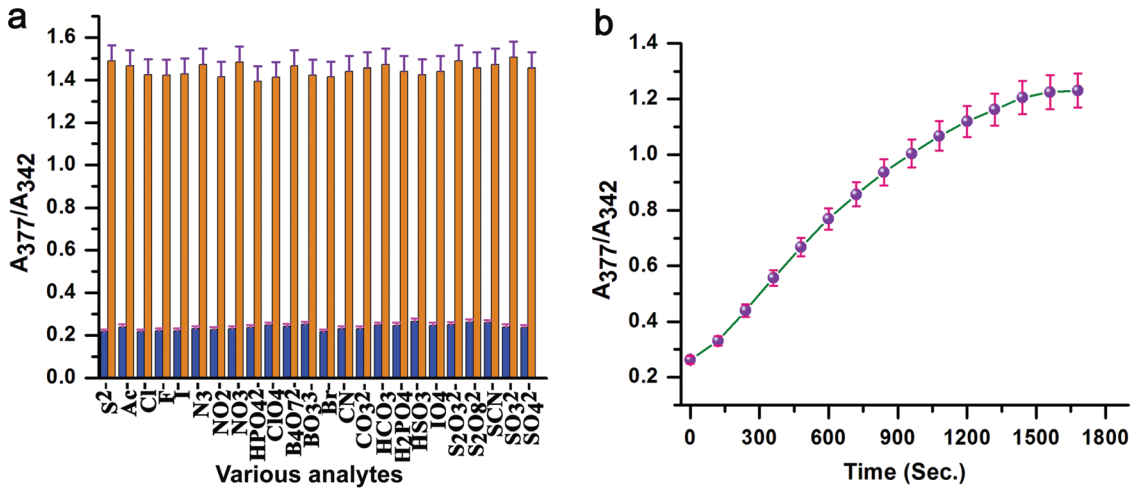

Fig. 2 (a) Absorbance ratio (A_{377}/A_{342}) of BER-S (10 μM) to various anions in CP buffer (10 mM, pH = 7.2). The blue bars represent the absorbance ratio of the probe in the presence of anions (each of 25 μM). The orange bars signify the changes of the ratios that occur upon the consequent addition of 25 μM of S^{2-} to the above solution, (b) time-dependent absorbance ratio (A_{377}/A_{342}) of BER-S (10 μM) with sulfide anions (25 μM) in CP buffer solution.

attack selectively sulfonate linkages. Thus the above result indicates that BER-S could specifically detect S^{2-} among the other anions.

Additionally, we also performed an ambitious experiment where the absorbance ratio (A_{377}/A_{342}) after the addition of S^{2-} in the presence other ions in BER-S solution was compared to that of the absorbance ratio (A_{377}/A_{342}) in the presence of S^{2-} anions only (Fig. 2a). Therefore, the colorimetric detection of S^{2-} by BER-S could withstand any interfering effects by other competitive anions.

3.2.4. Kinetics study. We also performed a kinetics study of BER-S (10 μM) upon the addition of S^{2-} to scrutinize the time required for nucleophilic attack by S^{2-} to sulfonate linkages in CP buffer solution (pH = 7.2). In this experiment, a stock solution containing BER-S and S^{2-} (1 : 2.5 equiv.) was shaken well before the spectral measurement and accordingly the absorption ratio (A_{377}/A_{342}) at 120 s intervals was measured. The result showed that the absorption ratio gradually increased and attained the highest value at 24 min, and after that no considerable increase in absorption ratio was observed (Fig. 2b). Therefore, the probe could detect S^{2-} after 24 min of its addition.

3.2.5. The pH stability. In consideration of whether our probe could also be useful with environmental and biological systems, we further examined the influence of pH toward the colorimetric detection of S^{2-} by BER-S. We found that the absorption ratio (A_{377}/A_{342}) of BER-S (10 μM) was more or less same for a wide range of pH (4–10), and consequently in the presence of S^{2-}, the absorption ratio (A_{377}/A_{342}) was nearly the same in the pH range 4–10 (Fig. S8, ESI†). The result indicates that the BER-S could be applied to a wide range of pHs for the selective detection of S^{2-}. Thus, we used pH 7.2 (near neutral pH) in the whole experimental procedures for the detection of S^{2-}, as this is very necessary for proving the environmental and biological applicability of the probe.

3.3. CT-DNA binding affinities studies by spectroscopic analysis

As our synthesized probe BER-S could detect sulfide anions in DNA-binding situations, the DNA-binding aspects and how the binding situation facilitates the detection of S^{2-} were also investigated.

3.3.1. Absorption and emission spectral studies. The binding of BER-S with CT-DNA was mainly investigated by an absorption spectroscopy titration methodology. In absorbance titration, significant bathochromic (342 nm to 347 nm) and hypochromic shifts (30.85%) were observed with three isosbestic points clearly visible (Fig. S1a, ESI†), which revealed a strong intermolecular association. We also investigated the DNA-binding affinity of BER-S *via* emission spectroscopy. Accordingly, upon excitation at 360 nm, the emission maxima shifted surprisingly from 490 nm to 530 nm, and the fluorescence intensity increased remarkably upon binding with DNA up to saturation (Fig. S1b, ESI†). Such a huge shift in the emission maxima of around 40 nm with enhanced intensity indicated a strong binding efficacy. The intrinsic binding affinity (K_i) and numbers of base pairs excluded by the binding of single alkaloid molecules (n) were obtained by analysis using McGhee–von Hippel's non-cooperative model of binding (Table S2, ESI†). The binding constant K_i was 3.6×10^5 M^{-1}, *i.e.*, greater than that of the parent berberine.[58] Details of the CT-DNA binding studies are incorporated in the ESI.†

3.4. Elucidation of the mode of binding of the analogue BER-S

3.4.1. By fluorescence quenching and viscosity measurement methods. Berberine is known to be a DNA intercalated alkaloid.[59] We are able to understand the mode of binding of the analogue through the fluorescence quenching method. In the fluorescence quenching method, an anionic quencher, *e.g.*, ferrocyanide ion, is used to distinguish between intercalation and the groove binding modes of a berberine analogue.[58] Further strong evidence about the mode of binding has come from viscosity measurements. In intercalation binding, the DNA helix lengthens and consequently the DNA viscosity increases, whereas in the case of partial or non-classical intercalation, the molecule can bend the DNA helix, shrinking its

effective length with an attendant decreases in its viscosity, and then the groove binding molecule does not change the viscosity of the DNA.[54] The results of these two methods strongly suggest that the mode of binding of the synthesized alkaloid to CT-DNA was mainly groove binding (Fig. S2a and b, ESI†). Details regarding the mode of binding of BER-S to DNA are described in the ESI.†

3.5. Spectral recognition study of S^{2-} by the BER-S/DNA complex

3.5.1. UV-vis spectroscopic recognition of S^{2-} by the BER-S/DNA complex. We studied the change in absorption spectra of BER-S/DNA complex in the presence of S^{2-}. Upon DNA binding, the absorption maxima of BER-S shifted from 342 nm to 347 nm (Fig. S10, ESI†), and thereafter, the introduction of S^{2-} elicited a red-shift from 347 nm to 368 nm, but in the presence of another anion, no perceptible spectral changes were observed, which accordingly tunes the colorimetric detection of S^{2-} by BER-S/DNA template (Fig. S11, ESI†). Thus, the BER-S/DNA complex could perform as an S^{2-} detector probe.

3.5.2. Fluorescence spectroscopic recognition of S^{2-} by the BER-S/DNA complex

3.5.2.1. Emission titration spectra. Further strong evidence for the detection of S^{2-} by the BER-S/DNA template comes from fluorescence spectroscopy. BER-S/DNA complex exhibited a weak fluorescence (ϕ = 0.0059) (Table S3, ESI†), but upon the successive addition of S^{2-}, the emission intensity at 530 nm increased gradually up to saturation (0 to 20 μM), and then after saturation the intensity was almost 10-fold higher compared to the complex (Fig. 3a), which made us consider that the BER-S/DNA complex is an excellent turn-on fluorescent sensor for S^{2-}. This is attributed to the fact the cleaved product berberrubine also interacts with DNA (berberrubine–DNA complex, ϕ = 0.02) (Table S3, ESI†), for which a remarkable change in fluorescence intensity was observed. Accordingly, we plotted the emission intensity at 530 nm (I_{530}) *vs.* concentration of S^{2-}, which reflected a nonlinear S-like curve and consequently a good linear relationship was noticed between I_{530} and S^{2-} concentration in the range 0.0–1.0 μM with a correlation coefficient value R^2 = 0.99816 (Fig. 3b). According to the IUPAC convention, the limit of detection value ($3\sigma/k$) was 46 nM, which was comparable and superior to previously reported work (Table 1) and much lower than the WHO-permitted S^{2-} concentration in drinking water. Thus, the BER-S/DNA complex could act as a superior fluorescence turn-on template for the detection of S^{2-}.

3.5.2.2. Comparison and discussion of the two LODs. The LOD values of S^{2-} in the colorimetric method without DNA and in the fluorometric method in the presence of DNA were 56 nM and 46 nM, respectively. As the fluorometric method has a lower LOD than the colorimetric method, we concluded that BER-S in the presence of DNA could act as a better probe for the detection of trace S^{2-} in real samples as well as in living cells. The detection of sulfides in the presence of DNA, *i.e.*, in the cell, is crucial as our body is easily contaminated by sulfide through drinking water as it is water soluble or through inhalation, which damages the cell. With this study, we became aware of the damaged cells due to sulfides compared to normal cells. In this platform, the sensing of sulfide in the presence of DNA is essential, and our synthesized analogue assured it could meet this purpose.

3.5.2.3. Selectivity and sensitivity. The excellent selectivity of the BER-S/DNA complex toward S^{2-} was examined by measuring the change in emission intensity (I_{530}) in the presence of S^{2-} and other relevant anions. Almost no change in emission intensity was seen with the addition of various anions as stated earlier, but surprisingly, upon the addition of S^{2-}, a vast increase in the fluorescence intensity at 530 nm was observed (Fig. S12, ESI†). Again, we checked the selectivity in the presence of various cations and other life elements and no observable change in fluorescence spectra was observed (Fig. S13 and S14, ESI†). Additionally, we also examined the change in I_{530} in the

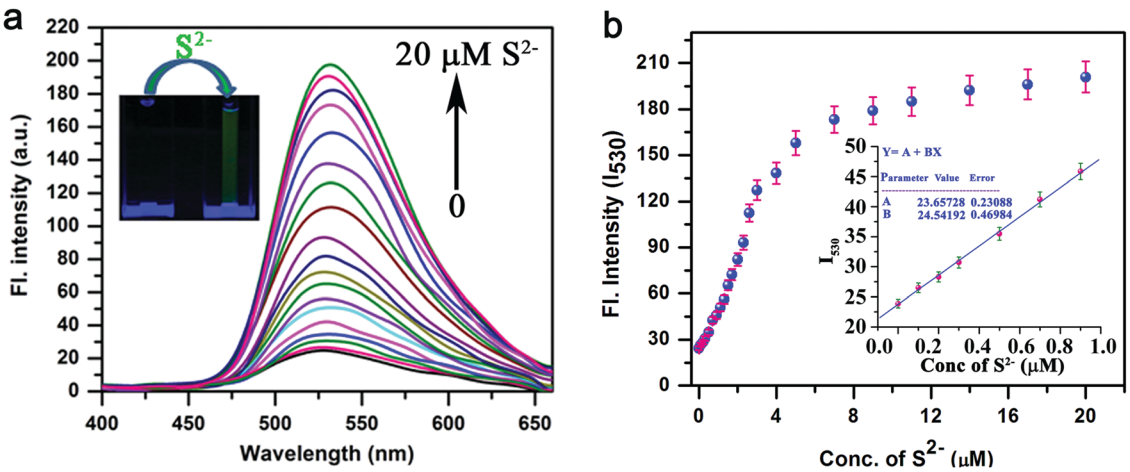

Fig. 3 (a) Fluorescence response of BER-S/DNA complex (probe = 10 μM, DNA = 150 μM) with increasing concentration of sulfide (0–2 equiv.). (b) Plot of fluorescence intensity at 530 nm of BER-S/DNA complex (probe = 10 μM, DNA = 150 μM) upon varied concentrations of sulfide (0–20 μM), λ_{ex} = 360 nm, λ_{em} = 530 nm, and the fl. intensity was linearly related to the concentration of sulfide (0.0–1.0 μM) in CP buffer solution (inset).

Table 1 Comparison of some published sensor-system for the detection of sulfide anion

Sensor system	Method	Solvent system	Linearity range	Detection limit	Ref.
Bimetallic terbium(III)/copper(II) complex	Fluorometric	10 mM HEPES buffer	0–2 μM	130 nM	18
A piperazine linker, an 8-aminoquinoline ligand	Fluorometric	HEPES buffer/ethanol (6 : 4 v/v)	0.5–8 μM	280 nM	19
7-Nitrobenz-2-oxa-1,3-diazole (NBD)	Fluorometric	HEPES aqueous buffer (THF–H_2O = 3 : 7)	0–3.0 μM	0.17 μM	21
2-Hydroxy-1-naphthaldehyde	Colorimetric	Bis–tris buffer/DMSO solution (v/v = 1 : 1)	Not mentioned	2.2 mM	22
Naphthalene diimide	Fluorometric	CH_3CN	Not mentioned	8.7 μM	40
Isophorone-based probe	Fluorometric	100% PBS buffer	0–200 μM	0.53 μM	46
dsDNA–CuNPs	Fluorometric	Aqueous	0–2 μM	80 nM	50
Berberine analogue	Colorimetric and fluorometric	100% CP buffer	0–1.0 μM	46 nM	This work

presence of biological thiols, *i.e.*, GSH, Cys, Hcy, Met, Cyt, and TBA. However, no remarkable change was observed in the fluorescence spectra in the presence of this thiol (Fig. 4a).

The above result is consistent with our expectation that the sulfonate linkage is selectively attacked by S^{2-} only and not by other ions, and also due to the greater nucleophilicity of S^{2-} compared with GSH, Cys, Hcy, Met, Cyt, and TBA. Thus the above result indicates that the BER-S/DNA complex could specifically detect S^{2-} among the other environmentally and biologically abundant anions.

3.5.2.4. Competitive ion study. To scrutinize whether the sensitivity of the BER-S/DNA complex toward sulfide anions could remain unchanged under the various potential competitive anions, 2 equiv. of sulfide anions were added to the BER-S/DNA (10 μM) in the presence of various relevant anions (2 equiv.) in pH 7.2 CP buffer solution (Fig. S15 and S16, ESI†). As shown in Fig. 4a, various biothiols have no interfering effect on the fluorometric detection of S^{2-}. Thus, the complex could perform as a good fluorescence turn-on S^{2-} detector template even involving various relevant potential anions and biothiols.

3.5.2.5. pH sensitivity. We further examined the effect of pH toward the fluorescence turn-on detection of S^{2-} by the BER-S/DNA complex, bearing in mind if our probe could also be applicable in a biological system. Tiny changes in emission intensity (I_{530}) of BER-S/DNA complex in the presence of S^{2-} were observed in the biological relevant pH range 4–9 (Fig. 4b). This result indicates that the BER-S/DNA complex is stable in the above pH range for the selective detection of S^{2-}. Thus, we used pH 7.2 for the fluorometric detection of S^{2-} by the BER-S/DNA complex, which is a significant pH for the biological application of the probe.

3.5.2.6. Time-dependent study. We also performed a time-dependent kinetics study to scrutinize the time required for the sensing response by the BER-S/DNA complex (10 μM). Upon the addition of 2 equiv. S^{2-} to the BER-S/DNA complex in CP buffer solution (pH = 7.2), the fluorescence intensity at 530 nm no more increased after 24 min (Fig. S17, ESI†). The above result indicates the complex could detect S^{2-} after 24 min of its addition.

3.5.3. Proposed sensing mechanism study

3.5.3.1. In colorimetric sensing. On the basis of the above sensing experiment, the sensing mechanism for the detection of S^{2-} was logically explained by the nucleophilic attack of S^{2-} toward the sulfonate linkage to produce the cleaved product berberrubine. For establishing the proposed sensing mechanism, we applied various analytical tools, like ESI-MS and IR spectroscopy. Further strong evidence came from the IR

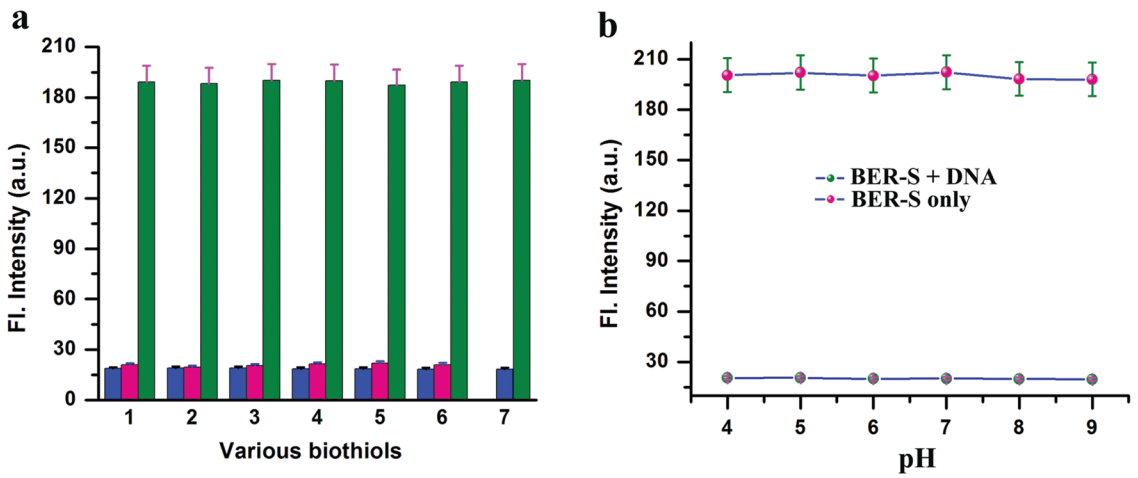

Fig. 4 (a) Selectivity and competitive study of BER-S + DNA complex in presence of biothiols (1: GSH, 2: Hcy, 3: Cys, 4: Met, 5: Cyt, 6: TBA, 7: S^{2-}). The blue bar represents the I_{530} of BER-S/DNA complex, red bars represent the I_{530} after the addition of biothiols and the olive bars represent the I_{530} of complex after the addition of S^{2-} in the presence of biothiols. (b) Fluorescence intensity (I_{530}) of BER-S/DNA complex and BER-S//DNA complex + S^{2-} at various pH values.

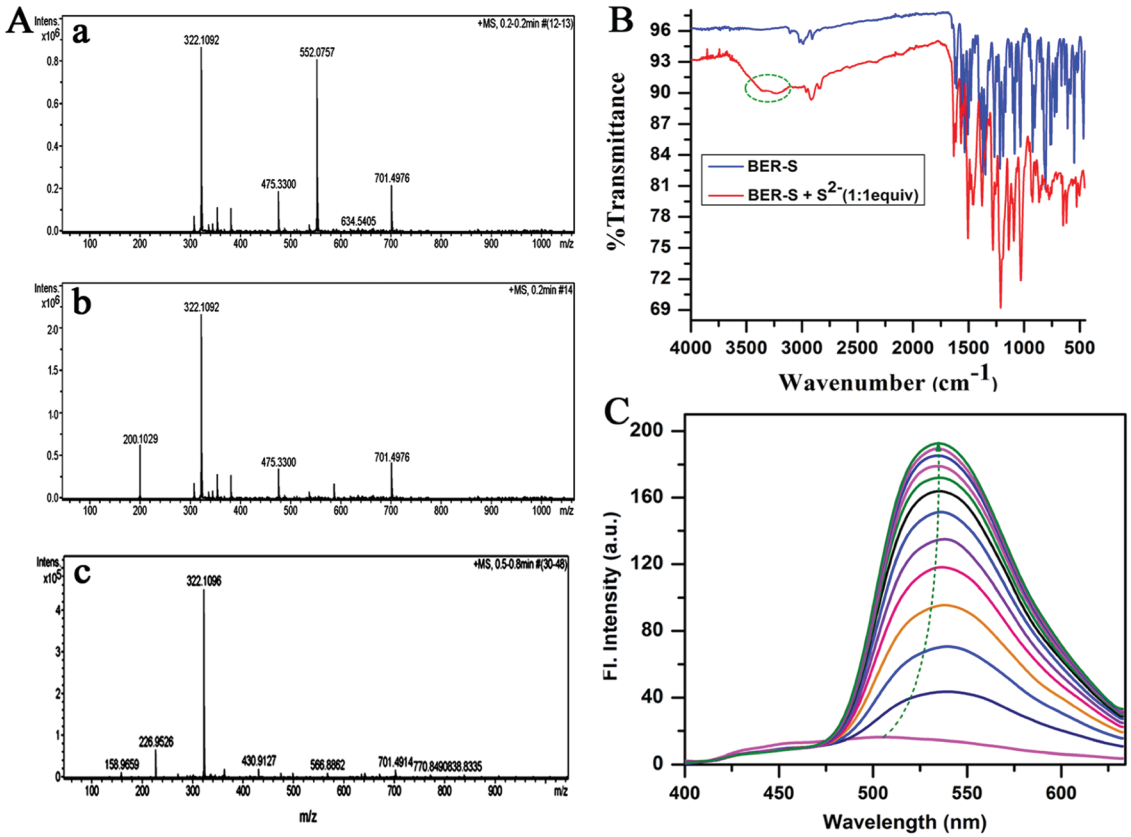

Fig. 5 (A) (a) HRLC-MS spectrum of BER-S + S^{2-} (1 : 1 equiv.), (b) BER-S + S^{2-} (1 : 2 equiv.), and (c) cleaved product, BER-OH. (B) IR spectra of the probe BER-S (blue), upon the addition of sulfide (red), a broad band appears at 3202 cm^{-1} assigned to the O–H stretching vibration. (C) In the presence of DNA, the fluorescence titration of BER-OH (10 μM) with increasing concentration of CT-DNA (up to 150 μM), λ_{ex} = 360 nm, λ_{em} = 530 nm.

spectral experiment. The IR spectra of BER-S after the addition of 3 equivalent S^{2-} showed a new broad peak at 3202 cm^{-1}, which was assigned to OH vibration stretching frequency (Fig. 5B), which further confirmed the generation of the hydroxyl group on berberine, *i.e.*, berberrubine. Further confirmation of the proposed mechanism came from the mass spectroscopic analysis. HRLC-MS of the solution containing BER-S/S^{2-} (1 : 1 equiv.) exhibited the two most abundant peaks with almost a 1 : 1 ratio at *m*/*z* 552 and 321, which indicated that both BER-S (*m*/*z* = 552) and the cleaved product BER-OH (*m*/*z* = 321) are present in solution at this stage (Fig. 5A(a)). Consequently, if we performed the mass spectra of the solution containing BER-S and S^{2-} (1 : 2.5 equiv.), only one abundant peak at *m*/*z* 321 (Fig. 5A(b)) was observed, corresponding to berberrubine (*m*/*z* = 321) (Fig. 5A(c)), *i.e.*, at this stage all BER-S molecules undergo nucleophilic reaction by S^{2-} anion. Thus, the IR and HRLC-MS analysis successfully established our proposed sensing mechanism.

3.5.3.2. In fluorometric sensing. The sensing mechanism is quite helpful in the presence of CT-DNA, and we can explain the sensing mechanism as follows. In the absence of DNA, the cleaved product BER-OH was confirmed by various analytical methods as stated previously. In the presence of DNA, the cleaved product BER-OH could also interact with DNA, which plays a decisive role in emission intensity enrichment upon the addition of sulfide. Accordingly, when we carried out the fluorescence titration of BER-S and BER-OH with increasing concentration of DNA, the maximum fluorescence intensity of BER-OH (Fig. 5C) was 10-fold greater than that of BER-S (Fig. 3a); comparable to that of the maximum fluorescence intensity obtained in the sulfide detection study (Fig. 3a). Thus, the above outcomes clarify the mechanism of sulfide detection in the presence of DNA.

3.6. Lifetime measurement

The lifetime data were measured by the time-correlated single photon counting (TCSPC) procedure using CP buffer of pH 7.2 at the excitation wavelength of 372 nm from a laser LED source. The time-resolved lifetime decay profile, $F(t)$ was studied by the following equation:

$$F(t) = \sum_{i=1}^{\alpha} a_i \exp(-t/\tau_i)$$

where n represents the number of segregate decay components, a_i and τ_i indicate an excited state fluorescence lifespan and the pre-exponential factors correspondingly correlated by means of the ith component.[60] The chi-square (χ^2) value indicates the best fitting. The consequential data were analyzed by EZ-time software. The TCSPC measurements were performed to realize the mechanism of the turn-on responses of the BER-S/DNA complex

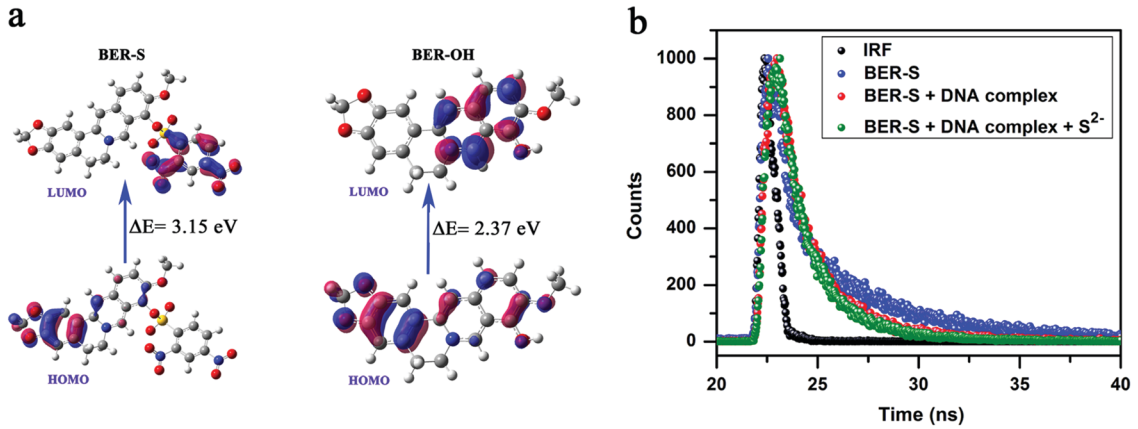

Fig. 6 (a) HOMO–LUMO energy level of probe BER-S and the corresponding product, BER-OH, (b) time-resolved fluorescence spectra of BER-S, BER-S/DNA complex, and BER-S/DNA + S^{2-} (2 equiv.), λ_{ex} = 372 nm and λ_{em} = 530 nm.

Table 2 Fluorescence lifetime data of BER-S, BER-S + DNA complex, and BER-S + DNA complex + S^{2-} (λ_{ex} = 372 nm) at pH 7.2

Entry	τ_1 (ps)	α_1	τ_2 (ns)	α_2	τ_{av} (ns)	χ^2
BER-S	418	0.78	4.05	0.22	1.217	1.18
BER-S + DNA-complex	806	0.67	2.48	0.33	1.358	1.17
BER-S + DNA-complex + 2.0 equiv. S^{2-}	637	0.61	2.06	0.39	1.192	1.11

toward S^{2-} ions (Fig. 6b). The average fluorescence lifetime (τ) of BER-S in CP buffer was 1.2 ns, while the average fluorescence lifetimes of the BER-S/DNA complex and BER-S/DNA complex + S^{2-} were 1.36 ns and 1.19 ns, respectively (Table 2). The fluorescence quantum yield of BER-S was 0.0005, whereas the quantum yield of the BER-S/DNA complex was 0.006, and accordingly an increase in the fluorescence lifetime of BER-S upon binding with DNA was expected, but only a little increment in lifetime was observed. The BER-S had two exponential decay natures, and it was observed that the lifetime of the major contributing exponential decay of 65% increased upon binding with DNA and that tuned the fluorescence intensity enhancement. Again, with the introduction of S^{2-} anions (2 equiv.) to the BER-S/DNA complex, the fluorescence quantum yield increased from 0.006 to 0.02, but the lifetime decreased (Table 2). This anomalous fluorescence property, *i.e.*, an increase in quantum yield but decrease in lifetime, may due to the enhanced local environment around the BER-S/DNA complex and higher emission rate constant.[61]

3.7. Density functional theory (DFT) calculations

We further scrutinized the change in electronic structure and observed the photophysical properties of BER-S upon the addition of sulfide anions *via* DFT study. The optimization of the synthesized analogue BER-S and its deprotected form, BER-OH, and DFT calculations were performed using the Gaussian 09 program at the CAM-B3LYP/6-31g(d,p) level. The resultant optimized geometries of BER-S and BER-OH are depicted in Fig. S19, ESI† and the frontier molecular orbital energies of HOMO and LUMO of BER-S and BER-OH were also calculated (Table S4, ESI†). The HOMO to LUMO energy gaps of BER-S and BER-OH were calculated as 3.15 eV and 2.37 eV, respectively (Fig. 6a). The product, after the addition of S^{2-} anions, BER-OH, had a lesser energy gap compared to BER-S, confirming the red-shift in UV-vis spectra, which clarified our experimental results (red-shift from 342 to 377 nm and 430 to 490 nm).

3.8. Analysis of real samples

The desired application of the probe (BER-S) was investigated by means of the quantitative detection of S^{2-} in waste water, tap water, and drinking water samples. The waste water samples were collected from a spinning mill near our university campus and used as usual. The experimental results (Table 3) indicated that the probe could recognize the spiked S^{2-} in real samples and the detected concentration concurred well with the added concentration, and the recoveries were acceptable too. This result revealed that the probe has proper exactness and accuracy for a quantitative finding of S^{2-} in water samples and has the potential to be used in water quality monitoring.

3.9. Living cell imaging studies

To further demonstrate the biological imaging application of BER-S in living cells, the cytotoxicity of the probe was evaluated first by the MTT [3-(4,5-dimethylthiazol-2-yl)-2,5-diphenyltetrazolium bromide] assay. The average value of four independent experiments was taken, and it was found that the compound had an IC_{50} value of 12.3 μM in A375 cells (Fig. S18, ESI†). Accordingly, we performed

Table 3 Detection of sulfide anions in real samples using the BER-S/DNA complex as a fluorescent probe

Samples	Na_2S added (μM)	Na_2S found (μM)	Recovery (%)	RSD (%, n = 3)
Waste water	1.5	1.49 ± 0.02	99.33	1.34
	2.1	2.04 ± 0.0264	97.14	1.29
	3.0	3.0267 ± 0.0472	100.88	1.58
Tap water	1.5	1.4633 ± 0.0416	97.33	2.84
	2.1	2.0767 ± 0.0252	98.57	1.21
	3.0	2.99 ± 0.0964	99.66	3.22
Drinking water	1.5	1.48 ± 0.0173	98.66	1.17
	2.1	2.1067 ± 0.0153	100.32	0.72
	3.0	2.98 ± 0.0360	99.33	1.21

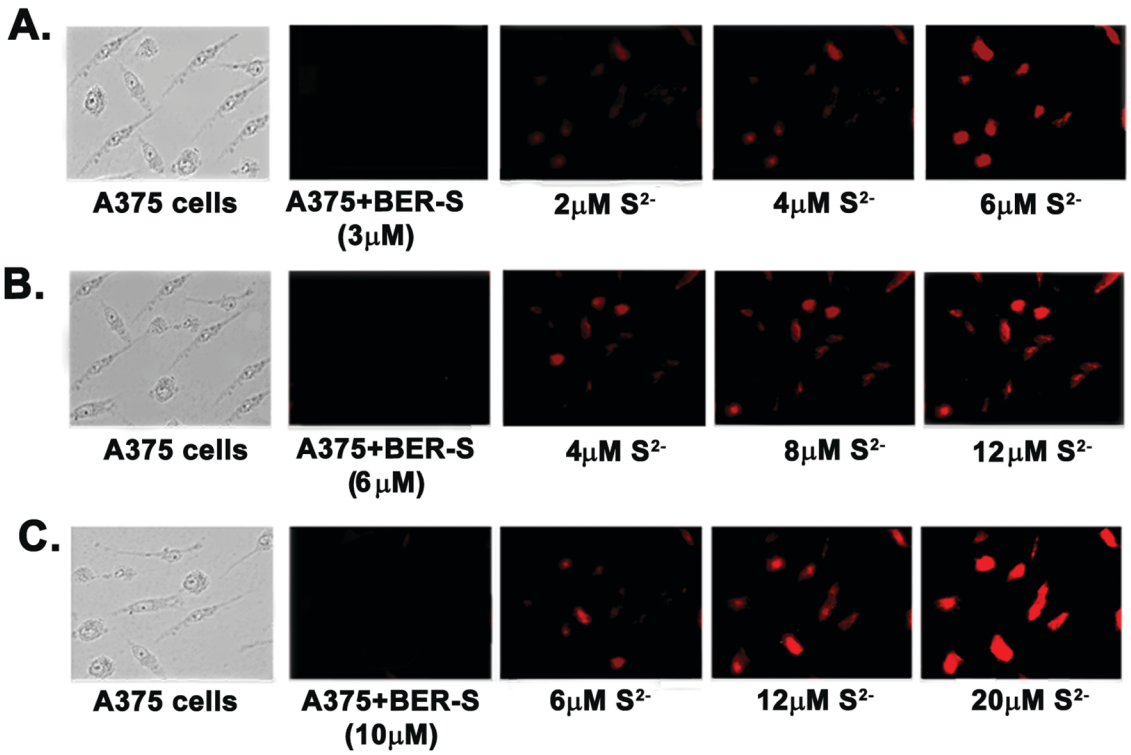

Fig. 7 (A) Fluorescence microscopic images of skin melanoma cells treated with 3 μM BER-S for 30 min and thereafter treated with various concentrations of S^{2-}. (B) Skin melanoma cells were treated with 6 μM BER-S for 30 min and then various concentrations of S^{2-}. (C) Skin melanoma BER-S were treated with 10 μM BER-S and then various concentrations of S^{2-} for 30 min, 200× magnification.

concentration variant living cell imaging to examine whether the probe could be used to detect sulfide in a biological system. The fluorescence microscopic image of a cell culture (2×10^4 cells per 35 mm culture plate) containing 3 μM BER-S after 30 min incubation showed no prominent fluorescence in the cells. After that, the cells were treated with various concentrations of S^{2-} up to 2 equivalents, and the results indicated that with increasing the concentration of S^{2-}, there was an increasing strong red fluorescence in the cells (Fig. 7A). Similarly, we performed the said experiment taking another two concentrations of BER-S (6 μM and 10 μM) and with increasing the sulfide concentration up to 2 equivalents in another two set of samples, and we got strong, eye-catching red fluorescence increasingly (Fig. 7B and C). From the above concentration variant cell imaging experiment, we concluded that our probe BER-S with a higher concentration (6 or 10 μM) could detect S^{2-} in living cells, and even a very low concentration of BER-S (3 μM) could detect a lower concentration of sulfide in living skin melanoma cells effectively. These results indicate that the probe had good cell permeability and the probe had a excellent capability for the fluorescence imaging of sulfide anions *in vivo*.

4. Conclusions

We developed a new probe BER-S based on isoquinoline alkaloid berberine with advantages of excellent water solubility. The probe BER-S could act as a colorimetric chemodosimeter in the absence of DNA and amazingly, as a fluorescent turn-on probe in the presence of DNA for aqueous sulfides and showed excellent selectivity and sensitivity over other analytes, including biothiols. Having no noticeable interference from other analytes, including biothiols, makes the BER-S and BER-S/DNA complex a proficient probe for sulfide detection. The limit of detection of BER-S and BER-S/DNA complex was as low as 46 nM and 56 nM, respectively, for the detection of sulfide anions, which are much lower than the extreme level of S^{2-} (15 μM) in drinking water acceptable by the WHO. The reaction-based sensing mechanism was well established *via* IR, HRMS, DFT, and fluorescence lifetime measurement. Real sample analysis and a live cell imaging study indicated the probe could be successfully used to detect S^{2-} in environmental water samples and living cells, respectively. Therefore, the BER-S and BER-S/DNA complex have potential applications in environmental and biological systems to assay S^{2-} and we deem that the results reported in this article could offer a new opportunity for designing and effortlessly synthesizing superb selective fluorescent chemodosimeters for S^{2-} in the presence of DNA.

Conflicts of interest

There are no conflicts to declare.

Acknowledgements

This study is financially assisted by the Department of Science and Technology (DST) Science and Engineering Research

Board (SERB), Govt. of India, No. SB/FT/CS-051/2013 (SERB/F/3694/2015-2016) and G. C. Jana gratefully acknowledges CSIR for Senior Research Fellowship (09/599(0058)/2014-EMR-1). M. Khatun and Sk. Nayim thanks to UGC for MANF fellowship. We are also obliged to USIC (Vidyasagar University), UGC-SAP DRS-II and DST-FIST New Delhi and for instrumental facilities.

References

1 (*a*) P. D. Beer and P. A. Gale, *Angew. Chem., Int. Ed.*, 2001, **40**, 486; (*b*) R. M. Máñez and F. Sancenón, *Chem. Rev.*, 2003, **103**, 4419.
2 Hydrogen Sulfide, World Health Organization, Geneva, 1981 (Environmental Health Criteria, No. 19).
3 (*a*) J. W. Morse and J. C. Cornwell, *Mar. Chem.*, 1987, **22**, 55; (*b*) T. Bagarinao, *Aquat. Toxicol.*, 1992, **24**, 21.
4 S. A. Patwardhan and S. M. Abhyankar, *Colourage*, 1988, **35**, 15.
5 P. Patnaik, *A Comprehensive Guide to the Hazardous Properties of Chemical Substances*, Wiley, New York, 3rd edn, 2007.
6 X. Shen, C. B. Pattillo, S. Pardue, S. C. Bir, R. Wang and C. G. Kevil, *Free Radical Biol. Med.*, 2011, **50**, 1021.
7 N. S. Lawrence, J. Davis and R. G. Compton, *Talanta*, 2000, **52**, 771.
8 C. Giuriati, S. Cavalli, A. Gorni, D. Badocco and P. Pastore, *J. Chromatogr. A*, 2004, **1023**, 105.
9 H.-H. Deng, G.-W. Wu, X.-Q. Lin, X.-W. Xu, A.-L. Liu, X.-H. Xia and W. Chen, *RSC Adv.*, 2015, **5**, 58574.
10 M. Colon, J. L. Todolí, M. Hidalgo and M. Iglesias, *Anal. Chim. Acta*, 2008, **609**, 160.
11 (*a*) L. Ferrer, G. de Armas, M. Miro, J. M. Estela and V. Cerda, *Talanta*, 2004, **64**, 1119; (*b*) D. Jimenez, R. Martínez-Manez, F. Sancenon, J. V. Ros-Lis, A. Benito and J. Soto, *J. Am. Chem. Soc.*, 2003, **125**, 9000.
12 Y. Jin, H. Wu, Y. Tian, L. Chen, J. Cheng and S. Bi, *Anal. Chem.*, 2007, **79**, 7176.
13 (*a*) M. F. Choi and P. Hawkins, *Anal. Chim. Acta*, 1997, **344**, 105; (*b*) M. A. Spaziani, J. L. Davis, M. Tinani and M. K. Carroll, *Analyst*, 1997, **122**, 1555.
14 J. Li, C. Yin and F. Huo, *RSC Adv.*, 2015, **5**(3), 2191.
15 Y. Yang, C. Yin, F. Huo, Y. Zhang and J. Chao, *Sens. Actuators, B*, 2014, **203**, 596.
16 Y. Yang, C. Yin, F. Huo, Y. Chu, H. Tong, J. Chao and F. Cheng, *Sens. Actuators, B*, 2013, **186**, 212.
17 Y. Yang, C. Yin, F. Huo, J. Chao and Y. Zhang, *Sens. Actuators, B*, 2014, **204**, 402.
18 M. L. Aulsebrook, S. Biswas, F. M. Leaver, M. R. Grace, B. Graham, A. M. Barrios and K. L. Tuck, *Chem. Commun.*, 2017, **53**, 4911.
19 X. Cao, W. Lin and L. He, *Org. Lett.*, 2011, **13**, 4716.
20 M. Wang, K. Li, J. Hou, M. Wu, Z. Huang and X. Yu, *J. Org. Chem.*, 2012, **77**, 8350.
21 Q. Meng, Y. Shi, C. Wang, H. Jia, X. Gao, R. Zhang, Y. Wang and Z. Zhang, *Org. Biomol. Chem.*, 2015, **13**, 2918.
22 S. M. Kim, M. Kang, I. Choi, J. J. Lee and C. Kim, *New J. Chem.*, 2016, **40**, 7768.
23 C. Kar, M. D. Adhikari, A. Ramesh and G. Das, *Inorg. Chem.*, 2013, **52**, 743.
24 S. Wang, S. Xu, G. Hu, X. Bai, T. D. James and L. Wang, *Anal. Chem.*, 2016, **88**, 1434.
25 F. J. Huo, J. Kang, C. Yin, J. Chao and Y. Zhang, *Sci. Rep.*, 2015, **5**, 8969.
26 J. Kang, F. Huo, P. Ning, X. Meng, J. Chao and C. Yin, *Sens. Actuators, B*, 2017, **250**, 342.
27 Q. Zhao, J. Kang, Y. Wen, F. Huo, Y. Zhang and C. Yin, *Spectrochim. Acta, Part A*, 2018, **189**, 8.
28 Y. L. Pak, J. Li, K. C. Ko, G. Kim, J. Y. Lee and J. Y. Yoon, *Anal. Chem.*, 2016, **88**, 5476.
29 L. Tang, Z. Zheng, K. Zhong and Y. Bian, *Tetrahedron Lett.*, 2016, **57**, 1361.
30 M. Ren, B. Deng, X. Kong, K. Zhou, K. Liu, G. Xu and W. Lin, *Chem. Commun.*, 2016, **52**, 6415.
31 B. Gu, N. X. Mi, Y. Y. Zhang, Y. Pen, H. T. Li and S. Z. Yao, *Anal. Chim. Acta*, 2015, **879**, 85.
32 F. Zheng, M. Wen, F. Zeng and S. Wu, *Sens. Actuators, B*, 2013, **188**, 1012.
33 Q. Zhao, C. Yin, J. Kang, Y. Wen and F. Huo, *Dyes Pigm.*, 2018, **159**, 166.
34 J. Kang, F. Huo and C. Yin, *Dyes Pigm.*, 2017, **146**, 287.
35 X. Xie, C. Yin, Y. Yue, J. Chao and F. Huo, *Sens. Actuators, B*, 2018, **277**, 647.
36 X. Yang, L. Wang, H. Xu and M. Zhao, *Anal. Chim. Acta*, 2009, **631**, 91.
37 R. Wang, F. Yu, L. Chen, H. Chen, L. Wang and W. Zhang, *Chem. Commun.*, 2012, **48**, 11757.
38 C. R. Liu, J. Pan, S. Li, Y. Zhao, L. Y. Wu, C. E. Berkman, A. R. Whorton and M. Xian, *Angew. Chem., Int. Ed.*, 2011, **50**, 10327.
39 P. Sathyadevi, Y. J. Chen, S. C. Wu, Y. H. Chen and Y. M. Wang, *Biosens. Bioelectron.*, 2015, **68**, 681.
40 L. Zong, M. Zhang, Y. Song, Y. Xie, J. Feng, Q. Li and Z. Li, *Sens. Actuators, B*, 2018, **257**, 882.
41 Y. Zhao, X. Zhu, H. Kan, W. Wang, B. Zhu, B. Du and X. Zhang, *Analyst*, 2012, **137**, 5576.
42 S. Chen, P. Hou and X. Z. Song, *Sens. Actuators, B*, 2015, **221**, 951.
43 J. M. Wang, H. Yu, Q. Li and S. J. Shao, *Talanta*, 2015, **144**, 763.
44 X. J. Yang, L. Q. Shen, H. B. Bao, X. X. Fang, J. W. Xu, Y. X. Zhao and W. Yang, *Sens. Actuators, B*, 2015, **220**, 1361.
45 Q. Huang, X. F. Yang and H. Li, *Dyes Pigm.*, 2013, **99**, 871.
46 F. Huo, Y. Zhang, P. Ning, X. Meng and C. Yi, *J. Mater. Chem. B*, 2017, **5**, 2798.
47 X. Li, J. Cheng, Y. L. Gon, B. Yang and Y. Z. Hu, *Biosens. Bioelectron.*, 2015, **65**, 302.
48 Z. J. Chen and H. W. Ai, *Biochemistry*, 2014, **53**, 5966.
49 W. Y. Chen, G. Y. Lan and H. T. Chang, *Anal. Chem.*, 2011, **83**, 9450.
50 J. Liu, J. Chen, Z. Fang and L. Zeng, *Analyst*, 2012, **137**, 5502.

51 G. C. Jana, Sk. Nayim, M. Khatun, S. Das, A. Patra, N. K. Sahoo, P. K. Jha, S. Mandal, K. Chaudhuri and M. Hossain, *ChemistrySelect*, 2017, **2**, 6519.
52 K. Bhadra, M. Maiti and G. Suresh Kumar, *Biochim. Biophys. Acta*, 2008, **1780**, 1054.
53 M. M. Islam, P. Pandya, S. Kumar and G. Suresh Kumar, *Mol. BioSyst.*, 2009, **5**, 244.
54 S. U. Rehman, T. Sarwar, M. A. Husain, H. M. Ishqi and M. Tabish, *PLoS One*, 2014, **9**, e93913.
55 J. D. McGhee and P. H. Von Hippel, *J. Mol. Biol.*, 1974, **86**, 469–489.
56 A. M. Brouwer, *Pure Appl. Chem.*, 2011, **83**, 2213.
57 Guidelines for Drinking-Water Quality, World Health Organization, Geneva, 3rd edn, 2004, http://www.who.int/water_sanitation_health/dwq/guidelines/en/.
58 D. Bhowmik, M. Hossain, F. Buzzetti, R. D'Auria, P. Lombardi and G. Suresh Kumar, *J. Phys. Chem. B*, 2012, **116**, 2314.
59 M. Ferraroni, C. Bazzicalupi, A. R. Bilia and P. Gratteri, *Chem. Commun.*, 2011, **47**, 4917.
60 J. R. Lakowicz, *Principles of Fluorescence Spectroscopy*, 3rd edn, Kluwer Academic Plenum Publishers, New York, 2006.
61 K. Ray, J. Zhang and J. R. Lakowicz, *Anal. Chem.*, 2008, **80**, 7313.